

A Compact Delay Model for OTS Devices

M. M. Al Chawa and R. Tetzlaff
Technische Universität Dresden
Dresden, Germany

Email: mohamad_moner.al_chawa@tu-dresden.de

D. Bedau, J. W. Reiner, D. A. Stewart and M. K. Grobis
Western Digital San Jose Research Center
San Jose, CA, USA

Email: daniel.bedau@wdc.com

Abstract—This paper presents a novel compact delay model of Ovonic Threshold Switch (OTS) devices that works efficiently for circuit simulations. The internal state variable of the two terminal devices is estimated using a delay system that uses a few electrical components related to a suggested equivalent circuit of the device. Finally, we tested the proposed model against measured data from devices fabricated by Western Digital Research.

I. INTRODUCTION

Chalcogenide alloys offer the possibility to fabricate a family of two terminal Ovonic Threshold Switch (OTS) devices. Usually, this kind of device presents a characteristic current-controlled negative differential resistance (NDR) on their DC $i-v$ curve. Due to this NDR, they exhibit an extremely fast and sharp switching between their on and off states, thus allowing them to be a good option for various applications: selectors for memory cells, fast switches, or neuromorphic computing [1]–[3].

Even though the exact mechanism behind the threshold switching is still under discussion, many models can accurately reproduce the phenomenological conduct of OTS devices [4], but they often lack efficiency when implemented on a circuit simulator. This is caused by the fact that these tools require a fast and precise model of the device described in a manner that suits an analogue simulation pipeline, including continuous derivatives. There is thus a compromise between the complexity that arises from the actual physical device and the required model accuracy. The capability of circuit simulation suites to run complicated models represents a challenge, that has been usually handled by the memristor device modelling community by using the classical current-voltage description [5], [6], or Chua's original proposition in flux and charge [7]–[11]. Any

of these approaches are equivalent [11], but following the most usual convention, we will use current and voltage in this work.

Usual methods model the charge carrier dynamics utilising transport models [12], [13] that are described by differential equations. These physics-based models tend to be complicated, cannot be directly implemented in circuit simulators, and do not sufficiently serve as compact models for circuit simulations. An illustration of a non-physical model of a nano two-terminal device, ReRAM, for low computational cost as an alternative model, has been demonstrated in [26]. However, in this work, the proposed model can be implemented in SPICE. Furthermore, a mathematical description of the equivalent circuit was obtained. The internal state variable, which controls the behaviour of the device, was extracted to get a compact model for OTS devices. Finally, this model was tested to fit $i-v$ experimental data of a physical OTS device fabricated by Western Digital Research.

II. MODEL DESCRIPTION AND IMPLEMENTATION

A. OTS Equivalent Circuit

We have built an equivalent circuit for the OTS device shown in Fig. 1. The circuit includes five junctions. A serial junction, J_s , and a parallel junction, J_p . Each junction consists of a diode and a capacitance in parallel. The other three junctions [25], J_1 , J_2 , and J_3 . Individually, the junction consists of a diode, a capacitance, and a current source in parallel. The diode is equal to the DC characteristic of the p-n junction current according to

$$I_J = \frac{I_s}{\alpha} \cdot (e^{v_J/V_T} - 1) \quad (1)$$

where,

$$\alpha = \frac{\beta}{1 + \beta} \quad (2)$$

V_T is the thermal voltage kT/q ($26mV$ at $300K$), and I_s is the reverse saturation current. The current source is described as

$$\alpha \cdot I_J \quad (3)$$

The capacitance $C_{total} = C_j + C_d$ involves a junction capacitance and a diffusion capacitance for each P-N junction (shown in Fig. 1), and both capacitances are voltage-dependent. We treat these junctions as Schottky junctions with the capacitance determined as [18]

$$C_j = \frac{C_{j0}}{(1 - v_c/v_j)^M}, \quad (4)$$

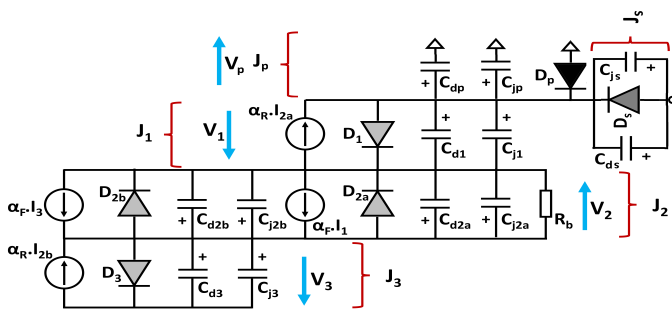
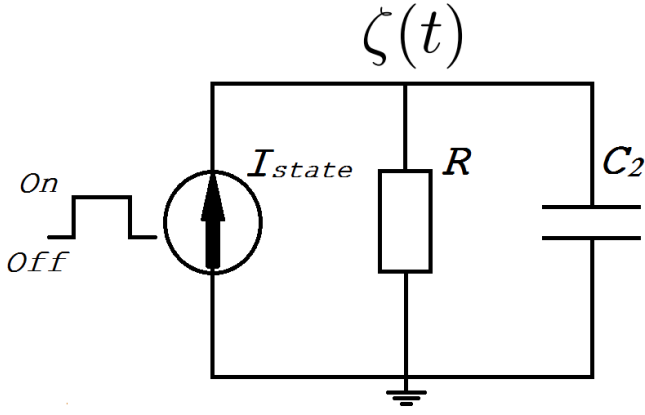
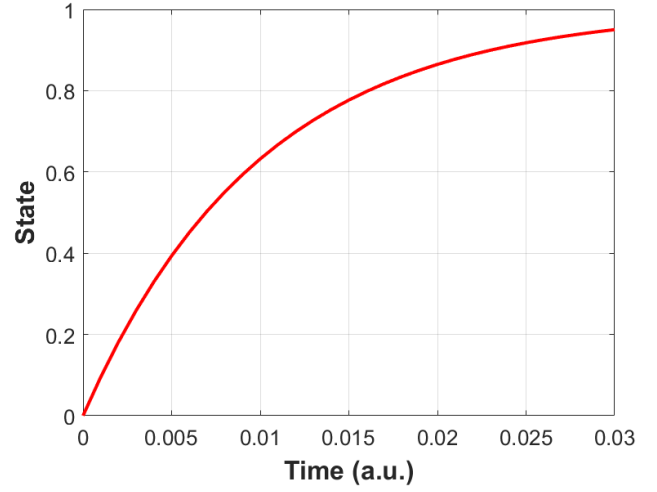


Figure 1: OTS cell equivalent circuit.

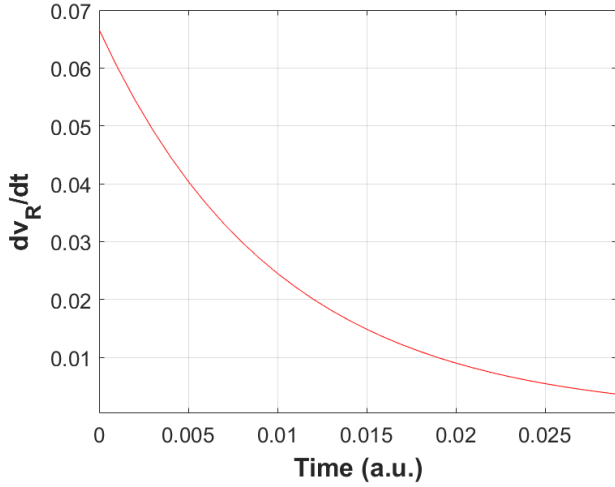


(a)

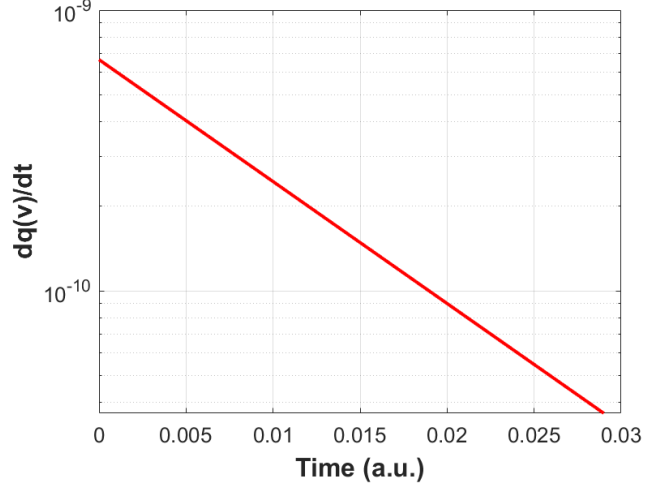


(b)

Figure 2: The Delay model extracted from J_2 in Fig. 1 to obtain the internal state variable. (a) The proposed circuit related to the J_2 : $C_2 = 10nF$, $R_b = 1M\Omega$ and $I_{state} = 1\mu A$; (b) The values of the internal state variable (voltage drop across the circuit in Fig. 2a) vs. time (a.u.).



(a)



(b)

Figure 3: (a) Derivative of the internal voltage drop v_R across the J_2 ($K = 0.7$); (b) Capacitive current through J_2 ($v \approx v_R$) in (10) considering a linear capacitor approximation, ($C \approx 10nF$).

where C_{j0} is the zero-bias capacitance, v_j is the built-in potential, and M corresponds to an experimental coefficient. The diffusion capacitance represents the minority carrier charge and is taken into account as

$$C_d \approx \Sigma \tau_j \frac{I_j}{V_T} \quad (5)$$

It is obvious that the proposed OTS equivalent circuit can be implemented and run in a circuit simulator.

B. Internal State Variable

The behaviour of the two terminals OTS device is a function of the internal state variable. This state variable has been

modelled as a delay function which goes from 0 to 1, and represents the switching of the state between its off and on values, respectively, as shown in Fig. 2a. The delay model has been constructed as the circuit shown in Fig. 1 employing a few elements linked to the second junction. The capacitor C_2 is common for all the capacitors present in parallel in the second junction J_2 . The resistor R_2 is related to the diodes and internal bias resistor, while the current source I_{State} is connected to the current sources in Fig. 1. The current source in Fig 2a is defined as two different values: it is assigned to $1\mu A$ when the voltage across the device overreaches or catches the threshold voltage, v_{th} (where i_{th} is the corresponding

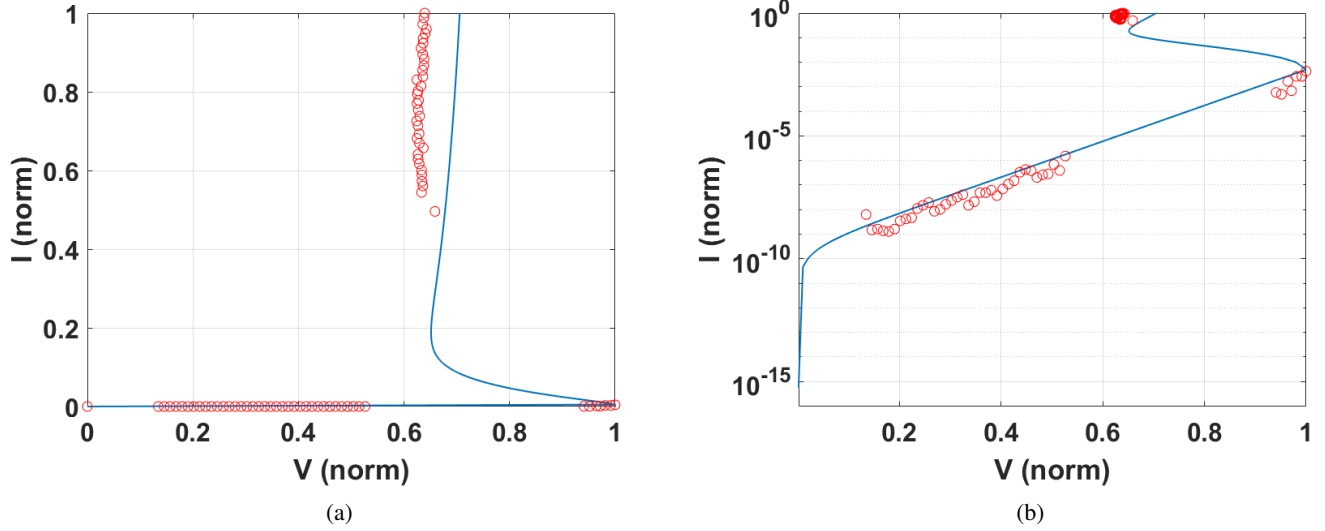


Figure 4: $i-v$ curve, red dots are (normalized) experimental data (symbols) and modeled using (14) (blue line) for OTS devices. The devices and experimental measurements obtained by Western Digital Research [25].

current). Otherwise, the value of the current source is zero when the voltage across the device falls under the threshold voltage. Applying KCL, the delay model can be described as

$$I_{State} = \frac{v_R}{R_2} + C_2 \cdot \frac{dv_R}{dt} \quad (6)$$

Let us suppose an internal state variable (in Volt), $State$ or $\zeta \in [0, 1]$, which can be obtained by solving the last equation as follows

$$\zeta(t) = I_{State} \cdot R_2 - e^{-\frac{t}{R_2 C_2}} \quad (7)$$

The plot of (7) is shown in Fig. 2b. Assuming a scaling factor K , the internal voltage drop across the J_2 can be expressed as

$$v_R = K \cdot \zeta \quad (8)$$

Fig. 3a illustrates the derivative of the last equation which represents the derivative of the internal voltage drop across the bias resistor.

C. Model Implementation

The proposed equivalent circuit in Fig. 1 can be implemented and run in a circuit simulator, which expects the behaviour by solving a mathematical model of the equivalent circuit. The model involves the compact models of the elements and their topological connectivity that form the circuit, including the capacitance. The dynamic of the mathematical model of the circuit is provided by [17], [25]

$$i(v) = \frac{dq(v)}{dt} + f(v) \quad (9)$$

where f is the currents passing through static branches of the equivalent circuit, and dq/dt is the (capacitive) current passing through time-dependent branches of the equivalent circuit. We already have defined the voltage drop across the second junction, J_2 , as the internal state variable of the device,

$v_2 = -v_R$. The current passing through the time-dependent branch connected to v_2 and J_2 is the main branch and can be given as

$$\frac{dq(v)}{dt} \approx \frac{dq(v_2)}{dt} = \frac{d[C_{total2} \cdot v_2]}{dt} \approx -C \cdot \frac{dv_R}{dt} \quad (10)$$

As an approximation, a linear capacitor has been considered $C_{total2} \approx C$, as we focus particularly on the modelling of $i-v$ snapback in this contribution. A better proper charge model described in (II-A) can be employed in this formulation without changing the equation structure. Fig. 3b illustrates the current passing through time-dependent branches of equivalent capacitance, $10nF$ in (10). Also, It should be known, that the voltage drop across the series junction J_s is negligible, $v_s = 0$. As a result of this, the voltage drop across the parallel junction J_p is approximated to $v_p = -v$, where v is the applied voltage across the OTS device. The first junction J_1 and the third junction J_3 are identical. So, the voltage drop across the first junction, J_1 , is equal to the voltage drop across the third junction, J_3 , i.e. $v_1 = v_3$. As a result of this, the voltage drop across the first junction, J_1 , or the third junction, J_3 , can be expressed as follows

$$v_1 = v_3 = \frac{v + v_R}{2} \quad (11)$$

On the other hand, the currents passing through the static branches can be obtained by using KCL as follows

$$f(v) = I_1 - \alpha_R \cdot I_2 - I_P \quad (12)$$

replacing (1), (2), and (11) in the last equation yielding to

$$f(v) = I_s \cdot \left[e^{v+v_R/2 \cdot V_T} \left(1 + \frac{1}{\beta_F} \right) - e^{-v_R/V_T} - \frac{1}{\beta_F} \right] - \left[\frac{I_s}{\alpha_R} \cdot (e^{-v/V_T} - 1) \right] \quad (13)$$

Table I: The parameter values used to fit experimental measurements in Fig. 4 using (14) .

Parameter	Value
I_s	$10^{-14} A$
β_F	250
α_R	1
V_T	$25.9mV$
K	0.7
I_{State}	$1\mu A$
R	$1M\Omega$
C	$10nF$
v_{th}	$2.4V$
i_{th}	$1\mu A$
R_b	$5k\Omega$

Eventually, the current i of the OTS device in (9) can be integrated into one formula using (10), and (13) as follows

$$i(v, v_R) = I_s \cdot [e^{v+v_R/2 \cdot v_T} (1 + \frac{1}{\beta_F}) - e^{-v_R/v_T} - \frac{1}{\beta_F} - \frac{1}{\alpha_R} \cdot (e^{-v/V_T} - 1)] - C \cdot \frac{d}{dt} v_R \quad (14)$$

We have tested the model with experimental data for a physical OTS device, which consisted of a Se-based OTS layer, approximately 15nm thick, with carbon electrodes. The OTS layer and electrodes were patterned into a pillar of approximately 40nm diameter. Data was obtained by using a voltage pulse, with an on-chip resistor used to limit the current after OTS thresholding. The parameter values for this fitting are listed in Table I. By overlaying the fitting line with the measurement, we show that the model reproduces the $i-v$ characteristics nicely, not just in the on and off states, but also in the snapback region as can be noticed in Fig. 4.

III. CONCLUSION

This work presents a novel compact delay model for OTS devices. The internal state variable of the two terminal devices is evaluated utilising a delay circuit with few electrical components related to the proposed equivalent circuit of the OTS cell. Lastly, we validated the model by fitting $i-v$ experimental data of the OTS devices fabricated by Western Digital Research.

REFERENCES

- [1] Tuma, T., Pantazi, A., Le Gallo, M., Sebastian, A. & Eleftheriou, E. Stochastic phase-change neurons. *Nature Nanotechnology*. **11**, 693-699 (2016)
- [2] Song, B., Xu, H., Liu, S., Liu, H., Liu, Q. & Li, Q. An ovonic threshold switching selector based on Se-rich GeSe chalcogenide. *Applied Physics A*. **125**, 1-6 (2019)
- [3] Read, J., Stewart, D., Reiner, J. & Terris, B. Evaluating Ovonic Threshold Switching Materials with Topological Constraint Theory. *ACS Applied Materials and Interfaces*. **13**, 37398-37411 (2021,8)
- [4] Zhu, M., Ren, K. & Song, Z. Ovonic Threshold Switching Selectors for Three-Dimensional Stackable Phase-Change Memory. *MRS Bulletin*. **44** pp. 715 (2019)
- [5] Demirkol, A., Ascoli, A., Messaris, I., Al Chawa, M. M., Tetzlaff, R. & Chua, L. A Compact and Continuous Reformulation of the Strachan TaOx Memristor Model With Improved Numerical Stability. *IEEE Transactions On Circuits And Systems I: Regular Papers*. **69**, 1266-1277 (2022)

- [6] Messaris, I., Brown, T., Demirkol, A., Ascoli, A., Al Chawa, M. M., Williams, R., Tetzlaff, R. & Chua, L. NbO2-Mott Memristor: A Circuit-Theoretic Investigation. *IEEE Transactions On Circuits And Systems I: Regular Papers*. **68**, 4979-4992 (2021)
- [7] Al Chawa, M. M., Benito, C. & Picos, R. A Simple Piecewise Model of Reset/Set Transitions in Bipolar ReRAM Memristive Devices. *IEEE Transactions On Circuits And Systems I: Regular Papers*. **65**, 3469-3480 (2018)
- [8] Al Chawa, M. M. & Picos, R. A Simple Quasi-Static Compact Model of Bipolar ReRAM Memristive Devices. *IEEE Transactions On Circuits And Systems II: Express Briefs*. **67**, 390-394 (2020)
- [9] Al Chawa, M. M., Picos, R. & Tetzlaff, R. A Compact Memristor Model for Neuromorphic ReRAM Devices in Flux-Charge Space. *IEEE Transactions On Circuits And Systems I: Regular Papers*. **68**, 3631-3641 (2021)
- [10] Al Chawa, M. M., Picos, R. & Tetzlaff, R. A Simple Memristor Model for Neuromorphic ReRAM Devices. *2020 IEEE International Symposium On Circuits And Systems (ISCAS)*. pp. 1-1 (2020)
- [11] Al Chawa, M. M., Picos, R., Roldan, J., Jimenez-Molinós, F., Villena, M. & Benito, C. Exploring resistive switching-based memristors in the charge-flux domain: A modeling approach. *International Journal Of Circuit Theory And Applications*. **46**, 29-38 (2018)
- [12] Degraeve, R., Ravsher, T., Kabuyanagi, S., Fantini, A., Clima, S., Garbin, D. & Kar, G. Modeling and spectroscopy of ovonic threshold switching defects. *2021 IEEE International Reliability Physics Symposium (IRPS)*. pp. 1-5 (2021)
- [13] Chen, Z., Tong, H., Cai, W., Wang, L. & Miao, X. Modeling and Simulations of the Integrated Device of Phase Change Memory and Ovonic Threshold Switch Selector With a Confined Structure. *IEEE Transactions On Electron Devices*. **68**, 1616-1621 (2021)
- [14] Eshraghian, J., Lin, Q., Wang, X., Iu, H., Hu, Q. & Tong, H. A Behavioral Model of Digital Resistive Switching for Systems Level DNN Acceleration. *IEEE Transactions On Circuits And Systems II: Express Briefs*. **67**, 956-960 (2020)
- [15] Adler, D., Shur, M., Silver, M. & Ovshinsky, S. Threshold switching in chalcogenide-glass thin films. *Journal Of Applied Physics*. **51**, 3289-3309 (1980)
- [16] Zalden, P., Shu, M., Chen, F., Wu, X., Zhu, Y., Wen, H., Johnston, S., Shen, Z., Landreman, P., Brongersma, M. & Others Picosecond electric-field-induced threshold switching in phase-change materials. *Physical Review Letters*. **117**, 067601 (2016)
- [17] McAndrew, C., Coram, G., Gullapalli, K., Jones, J., Nagel, L., Roy, A., Roychowdhury, J., Scholten, A., Smit, G., Wang, X. & Yoshitomi, S. Best Practices for Compact Modeling in Verilog-A. *IEEE Journal Of The Electron Devices Society*. **3**, 383-396 (2015)
- [18] Ida, R. & McAndrew, C. A physically-based behavioral snapback model. *Electrical Overstress / Electrostatic Discharge Symposium Proceedings 2012*. pp. 1-5 (2012)
- [19] Wang, T. & McAndrew, C. A Generic Formalism to Model ESD Snapback for Robust Circuit Simulation. *2018 40th Electrical Overstress/Electrostatic Discharge Symposium (EOS/ESD)*. pp. 1-8 (2018)
- [20] Chua, L. & Sing, Y. Nonlinear lumped-circuit model for scr. *IEE Journal On Electronic Circuits And Systems*. **3**, 5-14 (1979)
- [21] Chua, L. Device modeling via nonlinear circuit elements. *IEEE Transactions On Circuits And Systems*. **27**, 1014-1044 (1980)
- [22] Chua, L., Yu, J. & Yu, Y. Negative resistance devices. *International Journal Of Circuit Theory And Applications*. **11**, 161-186 (1983)
- [23] Chua, L. & Deng, A. Negative resistance devices: Part II. *International Journal Of Circuit Theory And Applications*. **12**, 337-373 (1984)
- [24] Ebers, J. & Moll, J. Large-signal behavior of junction transistors. *Proceedings Of The IRE*. **42**, 1761-1772 (1954)
- [25] Al Chawa, M., Bedau, D., Demirkol, A., Reiner, J., Stewart, D., Grobis, M. & Tetzlaff, R. A Compact Model of Threshold Switching Devices for Efficient Circuit Simulations. *IEEE Transactions On Circuits And Systems I: Regular Papers*. **70**, 4530-4538 (2023)
- [26] Al Chawa, M., Tetzlaff, R., Tjortjis, C., Stavrinides, S., De Benito, C. & Picos, R. A Behavioural Compact Model for Programmable Neuromorphic ReRAM. *Proceedings Of The 18th ACM International Symposium On Nanoscale Architectures*. (2024), <https://doi.org/10.1145/3611315.3633237>